A Pd_3L_6 Supramolecular Cage Incorporating Photoactive [2.2]Paracyclophane Units

*Diego Rota Martir,[a] Lucie Delforce,[a] David B. Cordes,[a] Alexandra M. Z. Slawin,[a] Stuart L. Warriner,[b] Denis Jacquemin,[c] and Eli Zysman-Colman[a]**

[a] Organic Semiconductor Centre, EaStCHEM School of Chemistry, University of St Andrews, St Andrews, Fife, UK, KY16 9ST, Fax: +44-1334 463808; Tel: +44-1334 463826; E-mail: eli.zysman-colman@st-andrews.ac.uk;
[b] School of Chemistry, University of Leeds, Woodhouse Lane, Leeds, LS2 9JT, UK.
[c] CESIAM Laboratory, UMR CNRS 6230, University of Nantes, 2, rue de la Houssinière, 44322 Nantes, Cedex 3, France.

Keywords: luminescent palladium cage, [2.2]paracyclophane ligands, supramolecular assembly.

Abstract. [2.2]Paracyclophane (pCp) scaffolds, unlike many □-conjugated building blocks, have been rarely explored in supramolecular self-assembly. Herein we report the synthesis and characterization of two ligands, **pCpd3py** and **pCpd4py**, composed of a pCp core functionalized at its 7- and 15-positions respectively with 3-pyridyl and 4-pyridyl units. The self-assembly of **pCpd4py** with Pd^{2+} metal ions afforded a $[Pd_3(\mathbf{pCpd4py})_6]^{6+}$ cage structure, **pCpd4py-Pd**, where the six **pCpd4py** ligands doubly bridge each edge of the Pd_3 triangular core. The ligand **pCpd4py** and the palladium cage **pCpd4py-Pd** have been characterized by NMR spectroscopy, ESI-MS spectrometry and X-ray diffraction analyses and their photophysical properties investigated by steady-state and time-resolved emission spectroscopy as well as Time-Dependent Density Functional Theory calculations.

Introduction.

The [2.2]paracyclophane (pCp) is a compact scaffold in which two benzene rings are rigidly held in phase with respect to each other by two para-disposed ethylene bridges.[1] Such a skeleton offers the unusual opportunity to study through-space (π-π transannular) and through-bond [σ(bridge)-π(annular)] electronic interactions that strongly perturb the chemical, optical, and electronic properties of the molecule.[2-3] In recent years synthetic methodologies to functionalise the pCp core have been developed and a variety of functional groups have been precisely positioned on the rings and bridges of pCp.[4-5] For example, Spuling, Sharma and co-workers[6] have recently reported the first examples of pCp compounds emitting via a thermally activated delayed fluorescence mechanism[7] due to the presence of a diphenylamine donor and a benzophenone acceptor units located on different decks of the pCp. Zafra and co-workers[8] reported a pCp skeleton functionalized with stilbenoid compounds possessing terminal donor-donor, acceptor-acceptor or donor-acceptor units that have the ability to promote charge and exciton migration. Park and co-workers[9] reported a pCp core functionalized with triarylamine moieties that served as an efficient hole-transporting material in hybrid perovskite solar cells.

The use of pCp as a photoactive scaffold in supramolecular self-assembly is, however, rare and almost exclusively limited to 1D-supramolecular architectures formed through transannular π-stacking or H-bonding interactions between pCp rings.[10] These 1D assemblies often exhibit a high electron delocalization across the entire supramolecular chains as a result of strong intermolecular π-stacking interactions between adjacent pCp units that produce materials with low-energy optical gaps, infrared emission, and high conductivity.[10]

There exist examples of 3D-photoactive cage assemblies that have been synthesized through integration of phosphorescent metal complexes,[11-12] porphyrins[13] or fluorescent aromatic compounds[14-16] into the ligand backbone of the metallosupramolecular architectures. These cages generally show red-shifted emission with lower photoluminescence quantum yields, Φ_{PL}, and shorter emission lifetimes, τ_{PL}, than the corresponding luminescent ligands[12] used in self-assembly. In the majority of the cases this is due to the formation of lower-energy charge-transfer states that involve both the photoactive ligand and the metal ions used as the structural component. To date, there are only three examples of pCp scaffolds used in metallosupramolecular self-assembly.[5,17-18] The first is a small PdL_2 macrocyclic structure where L represents pCp compounds functionalized with two ethynyl-2-pyridyl groups,[17] the second example reported by Lützen and co-workers,[5] describes a Pd_2L_4 cage structures incorporating chiral pCp ligands functionalized with 3-pyridyl units, while in the third most recent example by Lützen and co-workers,[19] a Fe_4L_6 helicate was formed upon mixing iron(II) triflate, 2-formylpyridine and a pCp ligand functionalized with aniline units (Figure **1**). Although these pCp ligands and their cage structures are photoactive, the emission properties were not discussed.

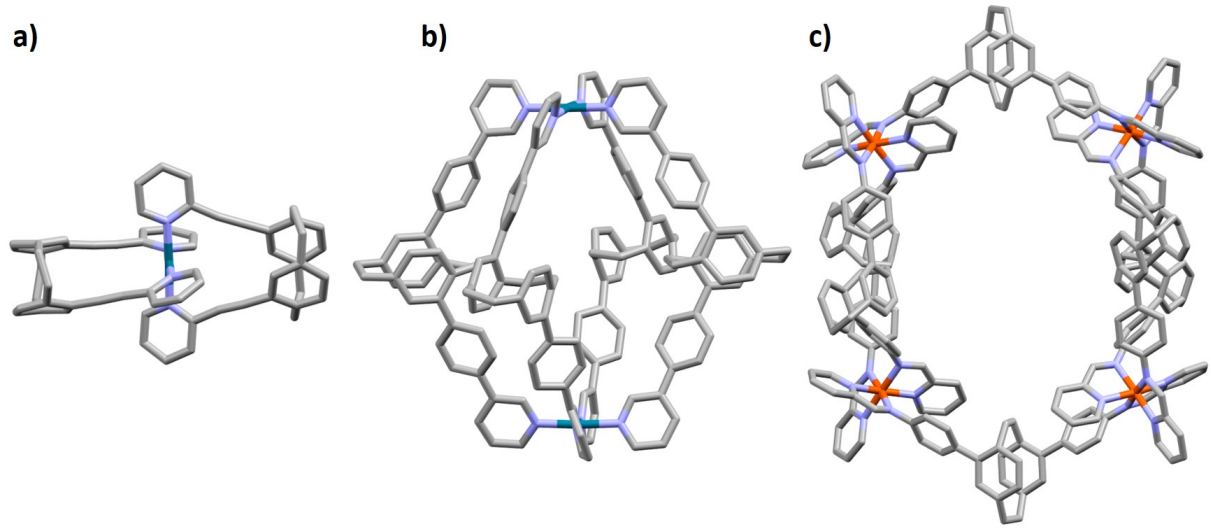

Figure **1**. Illustration of the X-ray crystal structures of **a)** PdL_2 macrocyclic structure[17], **b)** Pd_2L_4 cage structure[5] and **c)** Fe_4L_6 helicate[19] incorporating pCp compounds. Hydrogen atoms, solvent molecules and counterions have been omitted for clarity.

We report herein two pCp compounds functionalized at the 7- and 15-positions with 3- and 4-pyridyl coordinating units, **pCpd3py** and **pCpd4py** (Scheme **1**). The self-assembly of **pCp4py** with Pd^{2+} ions gives rise to a luminescent cage of composition $[Pd_3(\mathbf{pCpd4py})_6]^{6+}$, **pCpd4py-Pd** while under the same conditions the reaction of **pCpd3py** with Pd^{2+} produces multiple products, the structures of which could not be identified by ESI-mass spectrometry. As a result of the six photoactive pCp molecules rigidly assembled in the 3D cage-like structure, **pCpd4py-Pd** is emissive in both dichloromethane solution, λ_{PL}= 455 nm, and as a powder, λ_{PL}= 450 nm, with Φ_{PL} of 5% and 3%, respectively in solution and the solid state.

Results and Discussions.

The ligands **pCpd4py** and **pCpd3py** (Scheme **1**) were prepared in a single step *via* Suzuki-Miyaura palladium-catalysed cross-coupling of 7,15-dibromocyclophene with the corresponding pyridylboronic acid in yields of 75% and 70%, respectively. When **pCpd4py** and $[Pd(NCMe)_4](BF_4)_2$ were heated in a 2:1 ratio in DMSO-d_6 at 85°C for 12 h, the proton resonances associated with **pCpd4py** broadened and shifted downfield (Figure **2a**). The broad ^{1}H NMR signals are indicative of the formation of a large structure, the tumbling motion of which is very slow on the NMR timescale.[16] Evidence for the formation of a single species is confirmed by ^{1}H DOSY NMR spectroscopy where the diffusion coefficient, D, in DMSO-d_6 attains 9.2×10^{-11} m^2/s. The magnitude of D correlates to the presence of a larger

structure than the **pCpd4py** ligand, which shows a diffusion coefficient of 2.5×10^{-10} m^2/s (Figure **2b**). The corresponding hydrodynamic radius (r_s) of **pCpd4py-Pd** is estimated to be 12.2 Å (Table **S1**), larger than that of the Pd_2L_4 cage structure reported by Lützen and co-workers (10.4 Å, measured in DMSO-d_6, Figure **1b**) but smaller compared to the Fe_4L_6 helicate illustrated in Figure **1c** (14.0 Å, measured in CD_3CN).

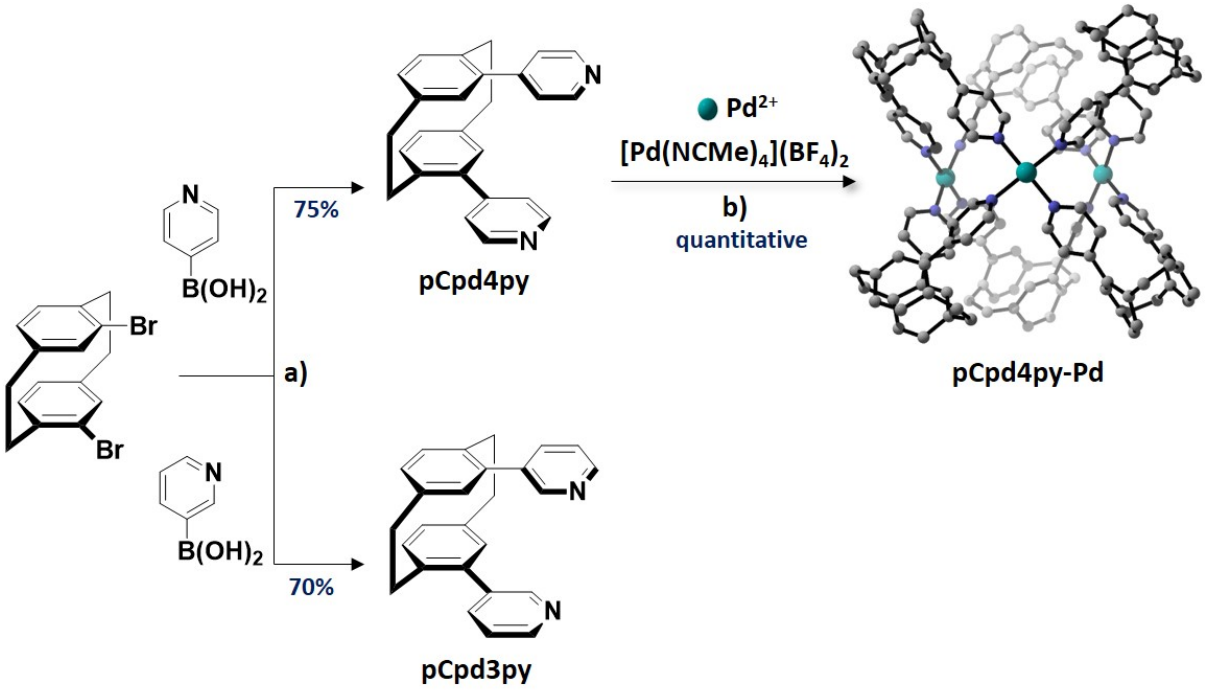

Scheme **1**. Synthesis of ligands **pCpd4py** and **pCpd3py** and cage **pCpd4py-Pd**. Reagents and conditions. [a]2.0 equiv. $CsCO_3$, 5 mol% $Pd(PPh_3)_4$, N_2, 1,4-dioxane/H_2O (4:1 v/v), 105 °C, 56 h; [b] DMSO, 85 °C, 12 h.

The composition of the assembly **pCpd4py-Pd** has been unequivocally established to be $[Pd_3(\mathbf{pCpd4py})_6](BF_4)_6$ by HR-ESI-mass spectrometry, showing isotopically resolved peaks for $[(\mathbf{pCpd4py\text{-}Pd})\text{-}(BF_4)_n]^{n+}$ (n = 2 - 5) (Figures **2** and **S10-S13**). The angle between the two 4-pyridyl coordinating motifs in **pCpd4py** is 50.2˚, which is adequate for the formation of a Pd_3L_6 cage.[20] Under similar reaction conditions, the self-assembly of **pCpd3py** with

$[Pd(NCMe)_4](BF_4)_2$ produced multiple products the structure of which could not be identified by ESI-MS.

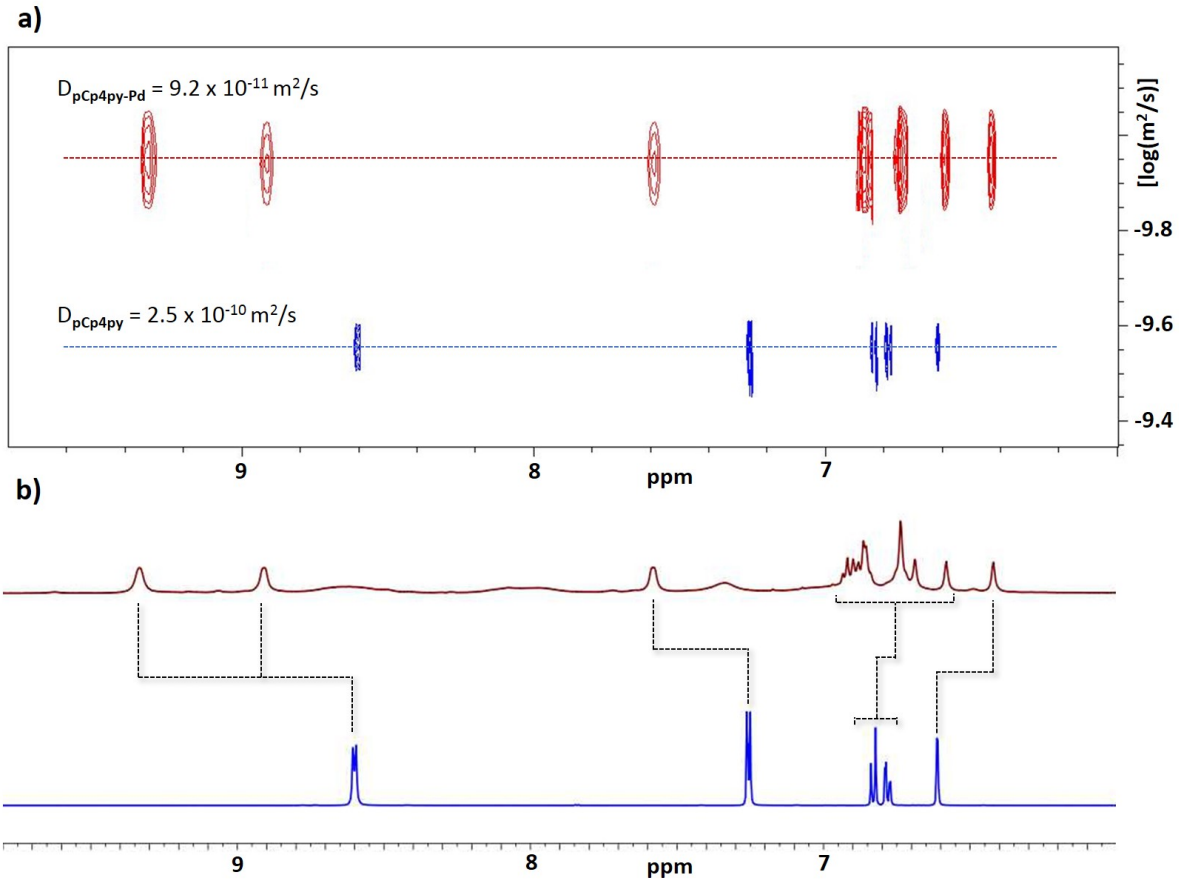

Figure **2**. **a)** ^{1}H NMR of **pCpd4py**, in blue and **pCpd4py-Pd**, in red. **c)**^{1}H DOSY NMR of **pCp4py**, in blue and **pCp4py-Pd**, in red. The NMR spectra were collected in DMSO-d_6 at 298 K.

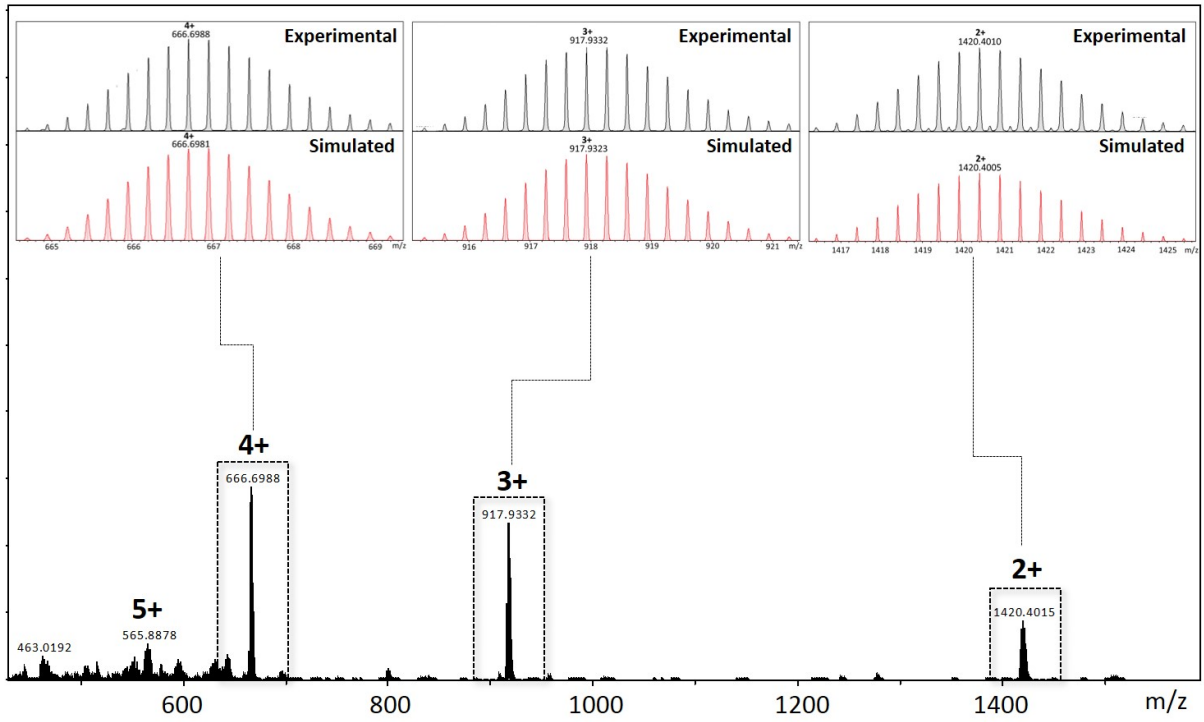

Figure **3**. ESI-MS of a DMSO-d_6 solution containing cage **pCpd4py-Pd**. Inserts show the measured (in black) and simulated (in red) isotope patterns for the 4+ (left), 3+ (center) and 2+ (right) charge states. Additional data is provided in the supporting information.

The X-ray structures of ligands **pCpd3py** and **pCpd4py** are shown in Figures **S14-S15** in the Supporting Information. The structure of **pCpd4py-Pd** was also unambiguously determined by X-ray crystallography (Figure **4**). Crystals suitable for X-ray analysis were grown by the slow diffusion of a 1:1 mixture of acetone-hexane into a DMSO-d_6 solution of **pCpd4py-Pd** (30 mM) over 5 days. The topology of **pCpd4py-Pd** resembles that reported by Fujita *et al.*[20] in which the cage is constructed such that two 4-pyridyl units of ligand **pCpd4py** doubly bridge adjacent Pd(II) centres, which are arranged in a regular triangle. Among Pd cages, this specific Pd_3L_6 arrangement is rare with only two other examples reported to date.[20-21] More generally, only a handful of metallocages of stoichiometry M_3L_6 have been reported.[22-24] The Pd···Pd distance around the cavity is 7.7 Å, and the inner cavity

diameter of the metallocage, determined from the distance between the centroid of the three palladiums, and a palladium, attains 8.8 Å. The longest external dimension of the cage is 18.0 Å (Figure **S7**). The inner diameter of cage **pCpd4py-Pd** is smaller to that of the Pd_3L_6 cage of Fujita *et al.*,[20] which showed a Pd···Pd distance of 8.7 Å.

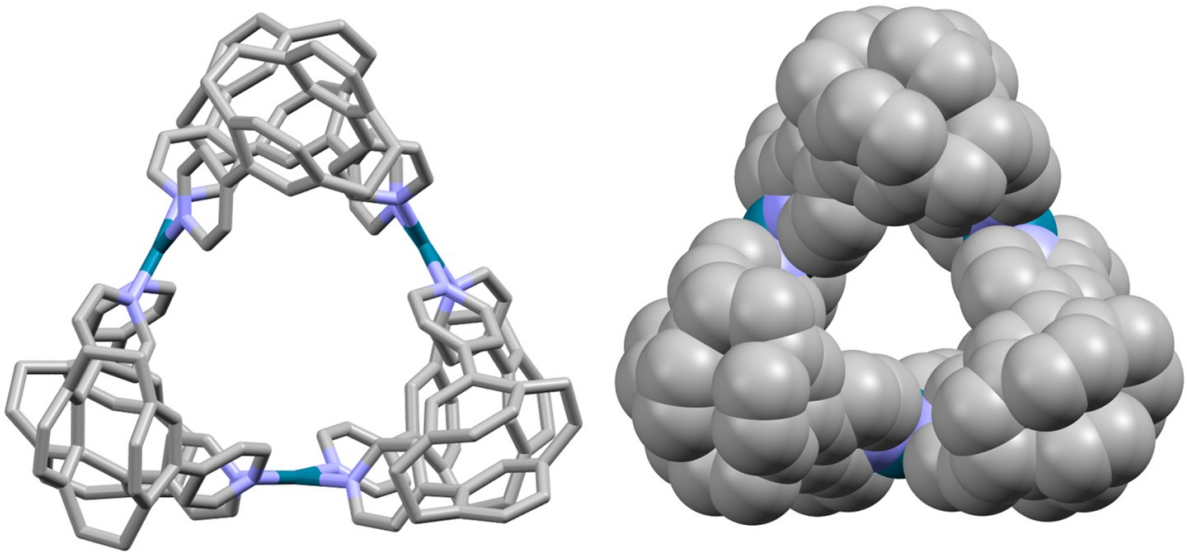

Figure **4**. Illustration of the X-ray crystal structure of **pCpd4py-Pd**. Capped sticks view (left) and space-filling view (right). Hydrogen atoms, solvent molecules and counterions have been omitted for clarity.

A racemic mixture of ligand **pCpd4py** containing both the enantiomers (S_p)-**pCpd4py** and (R_p)-**pCpd4py** was used to self-assemble cage **pCpd4py-Pd**. Circular Dichroism (CD) experiments reveals that cage **pCpd4py-Pd** is also formed as expected as a racemic mixture during the self-assembly process (Figure **S17**). However, this does not enable us to determine if **pCpd4py-Pd** is a racemic cage incorporating both (S_p)-**pCpd4py** and (R_p)-**pCpd4py** ligands in a statistical mixture, or whether there exists a racemic mixture of enantiopure cages. The X-ray structure of **pCp4py-Pd** reveals that each individual cage is enantiopure, but with a racemic mixture of cages occurring in individual crystals.

In DCM, ligands **pCpd4py** and **pCpd3py** exhibit absorption maxima at 289 nm and 328 nm for **pCpd4py** and at 280 nm with a shoulder at 328 nm for **pCpd3py**. The blue-shifted absorption bands of **pCpd3py** reflect the greater electron withdrawing character of the 3-pyridyl moiety compared to the 4-pyridyl moiety.[25] TD-PBE0 calculations (see the SI for details) return the three lowest vertical absorptions at 300 nm (*f*=0.004), 287 nm (*f*=0.140), and 276 nm (*f*=0.046) for **pCpd3py** and 306 nm (*f*=0.003), 287 nm (*f*=0.100), and 277 nm (*f*=0.098) for **pCpd4py**. These values are in reasonable agreement with experiment (Figure **5**) with first a weak band and next stronger absorptions. In both ligands, the two lowest transitions can be mainly ascribed to HOMO to LUMO and HOMO to LUMO+1 electronic promotions, respectively (Table **S3**). Both transitions do present a CT character from the phenyl rings to the pyridyl moieties (Figure **S24**)

The measured trends in their emission are similar with both showing broad and unstructured spectra characteristic of an intramolecular charge transfer state at λ_{PL}= 400 nm and λ_{PL}= 395 nm, respectively, for **pCpd4py** and **pCpd3py** and with Φ_{PL} of 12% and 14%, and τ_{PL} of 5 ns and 4 ns (Figure **5**). The powder emission of **pCpd4py** and **pCpd3py** is similar to those collected in DCM (for **pCpd4py**: λ_{PL}= 394 nm, Φ_{PL}= 9 %, τ_{PL}= 6 ns; for **pCpd3py**: λ_{PL}= 390 nm, Φ_{PL} = 11 %, τ_{PL}= 4 ns) (Table **1**). At the TD-PBE0 level, the computed emission wavelengths in DCM are 371 nm (*f*=0.006) and 375 nm (*f*=0.006) for **pCpd3py** and **pCpd4py**, respectively. The small oscillator strengths determined for these two emissions are consistent with the rather small quantum yield measured in both solution and powder.

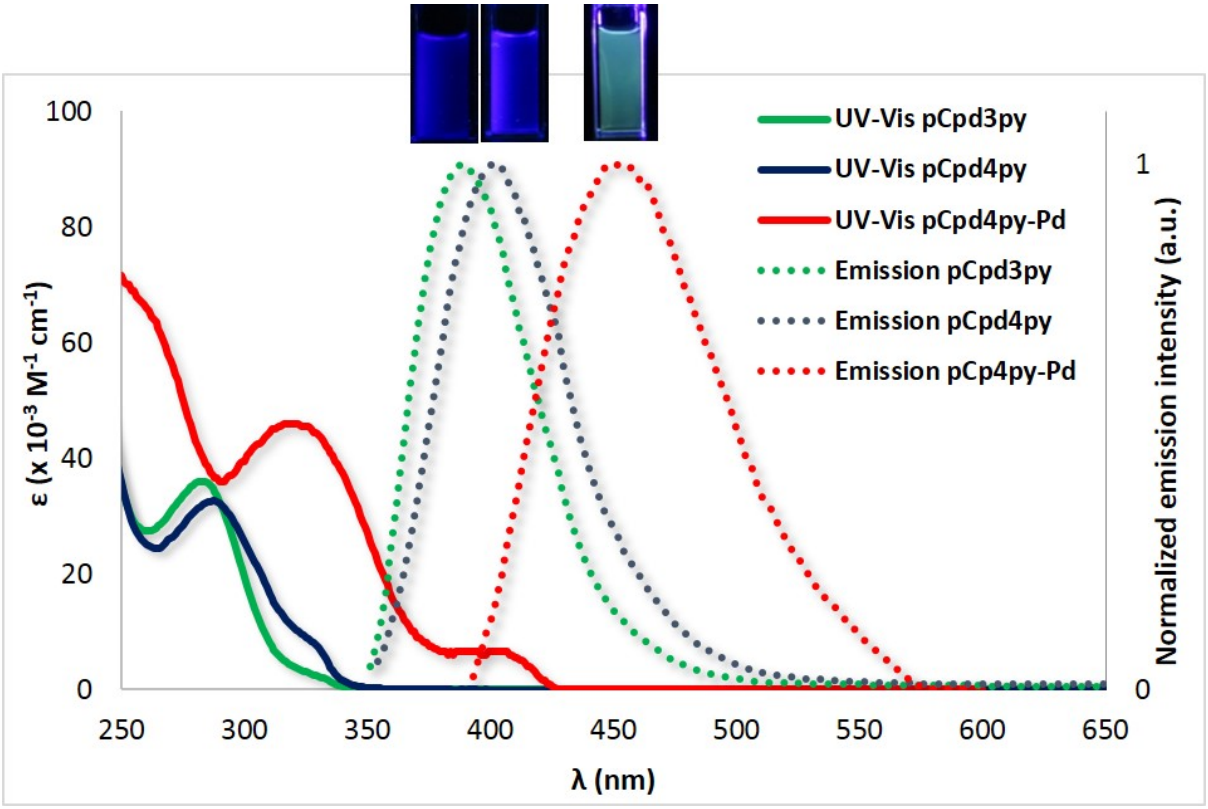

Figure **5**. UV-Vis absorption spectra of **pCp3dpy** (solid green line), **pCpd4py** (solid blue line) and **pCpd4py-Pd** (solid red line) collected in DCM at 298 K and normalized emission spectra of **pCpd3py** (dashed green line), **pCpd4py** (dashed blue line) and **pCpd4py-Pd** (dashed red line) collected in degassed DCM at 298 K (λ_{exc}= 340 nm). Photographs of DCM solutions of **pCpd3py, pCpd4py** and **pCpd4py-Pd** are shown in the inset.

The absorption spectrum of **pCpd4py-Pd** in DCM was red-shifted at 327 nm and 408 nm compare to that of **pCpd4py**. The higher energy band of **pCpd4py-Pd** at 327 nm can be attributed to the $^1\pi \rightarrow \pi^*$ ligand-centered transition localized on **pCpd4py**, while the broad, lower intensity band at 408 nm can be assigned to a charge transfer transition from the ligands **pCpd4py** to Pd centers (Ligand-to-Metal Charge Transfer). This evolution of the absorption spectra is consistent with TD-PBE0 results that also indicate the emergence of new transitions, e.g., a series of absorptions in the 365—377 nm domain, red-shifted by ca. +70 nm compared to the ligand, coherent with the experimental shift of ca. +80 nm (Table

S4). These transitions involve a CT from occupied orbitals localized on the phenyl rings of the ligands to unoccupied orbitals of the metallic cores (Figure **S25**). The emission profiles of cage **pCpd4py-Pd** in both DCM solution and as a powder are broader and red-shifted, respectively, at λ_{PL} = 455 nm and 450 nm, compared to those of **pCpd4py** (Table **1**). The photoluminescence quantum yields of **pCpd4py-Pd** are lower compared to those of **pCpd4py** at 5% in degassed DCM and 3% as a powder. The broad and red-shifted emission of cage **pCpd4py-Pd** as compared to **pCpd4py** results from the presence of the Pd(II) ions that effectively enhance the CT character of the lowest transitions, giving rise to smaller optical gaps.[11] However, similarly to that observed for other phosphorescent palladium cages incorporating emissive Ir(III) and Ru(II) metalloligands,[12] the Pd^{2+} ions do not completely quench the emission of **pCpd4py**. The lower Φ_{PL} values observed for **pCpd4py-Pd** compared to **pCpd4py** is likely due to the presence of several low-lying nearly perfectly dark states (see Table **S4** in the SI).

Table **1**. Photophysical properties of pCpd3py, pCpd4py and pCpd4py-Pd.

	λ_{PL}/ nm		Φ_{PL} / %		τ_{PL}/ ns	
	DCM[a]	powder[b]	DCM[c]	powder[b,d]	DCM[a]	powder[b,e]
pCpd3py	395	390	14	11	4	4
pCpd4py	400	394	12	9	5	6
pCpd4py-Pd	455	450	5	3	3	4

[a] Measurements in degassed DCM at 298 K (λ_{exc} = 340 nm). [b] measured as powder. [c]Φ_{PL} measurements were carried out in degassed DCM under nitrogen (λ_{exc} = 360 nm) using quinine sulfate as the external reference (Φ_{PL}= 54.6% in 0.5 M H_2SO_4 at 298 K).[26] [d] Values obtained using an integrating sphere. [e] λ_{exc} = 378 nm.

In conclusion, two deep-blue emissive [2.2]paracyclophanes molecules functionalized with 3-pyridyl and 4-pyridyl coordinating units, namely **pCpd3py** and **pCpd4py**, respectively, have been synthesized and characterized. The self-assembly of **pCpd4py** with Pd^{2+} ions

gives rise to a fluorescent cage of the composition of $[Pd_3(\mathbf{pCpd4py})_6](BF_4)_6$, **pCpd4py-Pd**. The cage has been comprehensively characterized by ^1H and ^1H-DOSY NMR spectroscopy and HR-ESI-MS and the structure of the cage was further elucidated by single crystal X-ray diffraction. The **pCpd4py-Pd** cage is emissive at 450 nm with Φ_{PL} of 5%. To the best of our knowledge, this is the first report that shows that supramolecular cages based on the rigid [2.2]paracyclophanes core scaffold are photoactive and can be potentially explored for optoelectronic applications. We therefore believe that the assembly of suitably functionalised pCp structures with metal ions as structural components opens up the possibility to prepare a wide range of supramolecular architectures such as coordination polymers, networks and macrocycles, that retain the optoelectronic properties of photoactive [2.2]paracyclophane molecules.

Supplementary materials

Experimental section, characterization of ligands **pCpd4py**, **pCpd3py** and cage **pCpd4py-Pd**, crystal structures (CCDC: 1951959-1951961), supplementary optoelectronic data and DFT and TD-DFT calculation details.

Acknowledgements

EZ-C acknowledges the University of St Andrews and EPSRC (EP/M02105X/1) for financial support. We thank the EPSRC UK National Mass Spectrometry Facility at Swansea University for analytical services. We thank Umicore AG for the gift of materials.

References

(1) Bahrin, L. G.; Sarbu, L. G.; Jones, P. G.; Birsa, L. M.; Hopf, H., [2.2]Paracyclophane-Bis(triazole) Systems: Synthesis and Photochemical Behavior. *Chem. Eur. J.* **2017**, *23*, 12338-12345.
(2) Kahnt, A.; Guldi, D. M.; de la Escosura, A.; Martínez-Díaz, M. V.; Torres, T., [2.2]Paracyclophane: a pseudoconjugated spacer for long-lived electron transfer in phthalocyanine–C60 dyads. *J. Mater. Chem.* **2008**, *18*, 77-82.
(3) Elacqua, E.; MacGillivray, L. R., From the Decks to the Bridges: Optoelectronics in [2.2]Paracyclophane Chemistry. *Eur. J. Org. Chem.* **2010**, *2010*, 6883-6894.
(4) Braun, C.; Nieger, M.; Bräse, S., Unprecedented One-Pot Reaction towards Chiral, Non-Racemic Copper(I) Complexes of [2.2]Paracyclophane-Based P,N-Ligands. *Chem. Eur. J.* **2017**, *23*, 16452-16455.
(5) Anhäuser, J.; Puttreddy, R.; Lorenz, Y.; Schneider, A.; Engeser, M.; Rissanen, K.; Lützen, A., Chiral self-sorting behaviour of [2.2]paracyclophane-based bis(pyridine) ligands. *Organic Chemistry Frontiers* **2019**, *6*, 1226-1235.
(6) Spuling, E.; Sharma, N.; Samuel, I. D. W.; Zysman-Colman, E.; Brase, S., (Deep) blue through-space conjugated TADF emitters based on [2.2]paracyclophanes. *Chem. Commun.* **2018**, *54*, 9278-9281.
(7) Wong, M. Y.; Zysman-Colman, E., Purely Organic Thermally Activated Delayed Fluorescence Materials for Organic Light-Emitting Diodes. *Adv Mater* **2017**, *29*, 1605444.
(8) Zafra, J. L.; Molina Ontoria, A.; Mayorga Burrezo, P.; Peña-Alvarez, M.; Samoc, M.; Szeremeta, J.; Ramírez, F. J.; Lovander, M. D.; Droske, C. J.; Pappenfus, T. M.; Echegoyen, L.; López Navarrete, J. T.; Martín, N.; Casado, J., Fingerprints of Through-Bond and Through-Space Exciton and Charge π-Electron Delocalization in Linearly Extended [2.2]Paracyclophanes. *J. Am. Chem. Soc.* **2017**, *139*, 3095-3105.
(9) Park, S.; Heo, J. H.; Cheon, C. H.; Kim, H.; Im, S. H.; Son, H. J., A [2,2]paracyclophane triarylamine-based hole-transporting material for high performance perovskite solar cells. *J. Mater. Chem. A* **2015**, *3*, 24215-24220.
(10) Fagnani, D. E.; Meese Jr., M. J.; Abboud, K. A.; Castellano, R. K., Homochiral [2.2]Paracyclophane Self-Assembly Promoted by Transannular Hydrogen Bonding. *Angew. Chem. Int. Ed.* **2016**, *55*, 10726-10731.
(11) Rota Martir, D.; Zysman-Colman, E., Supramolecular iridium(III) assemblies. *Coord. Chem. Rev.* **2018**, *364*, 86-117.
(12) Rota Martir, D.; Zysman-Colman, E., Photoactive supramolecular cages incorporating Ru(ii) and Ir(iii) metal complexes. *Chem. Commun.* **2019**, *55*, 139-158.
(13) Durot, S.; Taesch, J.; Heitz, V., Multiporphyrinic cages: architectures and functions. *Chem Rev* **2014**, *114*, 8542-8578.
(14) Kishi, N.; Akita, M.; Yoshizawa, M., Selective host-guest interactions of a transformable coordination capsule/tube with fullerenes. *Angew Chem Int Ed Engl* **2014**, *53*, 3604-3607.
(15) Frischmann, P. D.; Kunz, V.; Wurthner, F., Bright Fluorescence and Host-Guest Sensing with a Nanoscale M(4)L(6) Tetrahedron Accessed by Self-Assembly of Zinc-Imine Chelate Vertices and Perylene Bisimide Edges. *Angew Chem Int Ed Engl* **2015**, *54*, 7285-7289.
(16) Martir, D. R.; Pizzolante, A.; Escudero, D.; Jacquemin, D.; Warriner, S. L.; Zysman-Colman, E., Photoinduced Energy and Electron Transfer Between a Photoactive Cage Based on a Thermally Activate Delayed Fluorescence Ligand and Encapsulated Fluorescent Dyes. *ACS Applied Energy Materials* **2018**, *1*, 2971-2978.
(17) Meyer-Eppler, G.; Topić, F.; Schnakenburg, G.; Rissanen, K.; Lützen, A., Chiral Self-Sorting of trans-Chelating Chiral Ligands upon Formation of PdII Complexes. *Eur. J. Inorg. Chem.* **2014**, *2014*, 2495-2501.

(18) Gon, M.; Morisaki, Y.; Chujo, Y., A silver(i)-induced higher-ordered structure based on planar chiral tetrasubstituted [2.2]paracyclophane. *Chem. Commun.* **2017**, *53*, 8304-8307.
(19) Anhäuser, J.; Puttreddy, R.; Glanz, L.; Schneider, A.; Engeser, M.; Rissanen, K.; Lützen, A., Subcomponent self-assembly of a cyclic tetranuclear Fe(II) helicate in a highly diastereoselective self-sorting manner. *Chem. Eur. J.*, *0*.
(20) Suzuki, K.; Kawano, M.; Fujita, M., Solvato-controlled assembly of Pd3L6 and Pd4L8 coordination "boxes". *Angew Chem Int Ed Engl* **2007**, *46*, 2819-2822.
(21) Han, M.; Luo, Y.; Damaschke, B.; Gómez, L.; Ribas, X.; Jose, A.; Peretzki, P.; Seibt, M.; Clever, G. H., Light-Controlled Interconversion between a Self-Assembled Triangle and a Rhombicuboctahedral Sphere. *Angew. Chem. Int. Ed.* **2016**, *55*, 445-449.
(22) Zhang, T.; Zhou, L.-P.; Guo, X.-Q.; Cai, L.-X.; Sun, Q.-F., Adaptive self-assembly and induced-fit transformations of anion-binding metal-organic macrocycles. *Nature Communications* **2017**, *8*, 15898.
(23) Liu, Y.; Zhang, R.; He, C.; Dang, D.; Duan, C., A palladium(ii) triangle as building blocks of microporous molecular materials: structures and catalytic performance. *Chem. Commun.* **2010**, *46*, 746-748.
(24) Jurček, O.; Bonakdarzadeh, P.; Kalenius, E.; Linnanto, J. M.; Groessl, M.; Knochenmuss, R.; Ihalainen, J. A.; Rissanen, K., Superchiral Pd3L6 Coordination Complex and Its Reversible Structural Conversion into Pd3L3Cl6 Metallocycles. *Angew. Chem. Int. Ed.* **2015**, *54*, 15462-15467.
(25) Blanch, J. H., Determination of the Hammett substituent constants for the 2-, 3-, and 4-pyridyl and -pyridinium groups. *Journal of the Chemical Society B: Physical Organic* **1966**, 937-939.
(26) Melhuish, W. H., Quantum Efficiences Of Fluorescence Of Organic Substances: Effect Of Solvent And Concentration Of The Fluorescent Solute 1. *J. Phys. Chem.* **1961**, *65*, 229-235.